



## RESEARCH

WILEY

# Size and shape regulation during larval growth in the lepidopteran *Pieris brassicae*

Giuseppe Fusco | Emanuele Rigato | Arianna Springolo

Department of Biology, University of Padova, Padua, Italy

**Correspondence**

Giuseppe Fusco, Department of Biology, University of Padova, Padua, Italy.  
Email: [giuseppe.fusco@unipd.it](mailto:giuseppe.fusco@unipd.it)

**Funding information**

Italian Ministry of Education, University and Research (MIUR)

**Abstract**

By adopting a longitudinal study design and through geometric morphometrics methods, we investigated size and shape regulation in the head capsule during the larval development of the cabbage butterfly *Pieris brassicae* under laboratory conditions. We found evidence of size regulation by compensatory growth, although not equally effective in all larval stages. Size compensation is not attained through the regulation of developmental timing, but rather through the modulation of per-time growth rate. As for the shape, neither the variance of the symmetric component of shape, nor the level of fluctuating asymmetry show any evidence of increase across stages, either at the population or individual level, which is interpreted as a mark of ontogenetic shape regulation. In addition, also the geometry of individual asymmetry is basically conserved across stages. While providing specific documentation on the ontogeny of size and shape variation in this insect, this study may contribute to a more general understanding of developmental regulation and its influence on phenotypic evolution.

**KEYWORDS**

arthropods, compensatory growth, developmental stability, fluctuating asymmetry, geometric morphometrics

## 1 | INTRODUCTION

Size and shape are important fitness components along the whole ontogeny in most organisms, especially among multicellular eukaryotes, and are considered to be key determinants of several life history traits (Roff, 1992). Not surprisingly, the capacity of developmental systems and developmental processes for buffering against variation due to internal or external causes has been recorded in many taxa (Klingenberg, 2019), although the underlying mechanisms have been elucidated only in few models, in particular with reference to size (e.g., Nijhout & Callier, 2015).

In investigating size and shape regulative processes associated to growth, it is useful to introduce the concept

of *target ontogenetic trajectory* (Minelli & Fusco, 2013), which can be defined as the series of character states through all the developmental stages of an individual with a specific genotype in a specific environment, in the absence of any stochastic disturbance. This is an extension of the original concept of “target phenotype” (Klingenberg, 2019; Nijhout & Davidowitz, 2003), where a developmental trajectory is simply a more inclusive notion of the phenotype (Fusco, 2001). During development, body growth (or the growth of specific body parts) tends to depart from the target trajectory as a result of variation in the external factors that are known to influence growth rates (such as temperature, nutrition or parasitism; reviewed in Hartnoll, 1982), or because of developmental noise (Nijhout & Davidowitz, 2003).

However, the developmental systems of both animals and plants have been shown to incorporate controlling mechanisms that can buffer, at least to some extent, against the effects of different perturbing factors.

In arthropods, where size increase of exoskeletal structures occurs mainly in stepwise manner, paced by the moult cycle, *compensatory growth* (also termed *targeted growth* or *convergent growth*) occurs when individuals adjust their growth trajectories stage-by-stage, thus keeping their ontogenetic trajectory in size close to the target trajectory (Minelli & Fusco, 2013). In holometabolous insects, which have determinate growth, the level of compensation is reflected in the magnitude of size variation at the terminal reproductive stage (imago). Similarly, *ontogenetic shape regulation* occurs when individual trajectories in the shape space, eventually divided in their symmetric and asymmetric components, are buffered against possible deviations due to a diversity of potential sources of developmental disturbance.

Unfortunately, despite recent advances in the understanding of the molecular and physiological mechanisms that regulate body growth in arthropods, in a few model insects in particular (Grunert et al., 2015; Shingleton, 2010), observational data on the phenomena of size and shape regulation are relatively scarce. This limits the scope for comparative analyses in a phylogenetic context, and, in an evo-devo perspective, the possibility to assess the influence of developmental regulation on phenotypic evolution (Bruijning et al., 2020; Fusco & Minelli, 2010; Van Dongen, 2006).

Here, by adopting a longitudinal study-design, that is, by operating on a data set consisting of the measurements of the same individual in subsequent stages (Cock, 1966), and through geometric morphometrics methods (Bookstein, 1991), we investigate the regulation of size and shape during larval development of the cabbage butterfly *Pieris brassicae* (Linnaeus, 1758) under laboratory conditions. Shape analysis is divided in the analysis of between-individual variation in the symmetric shape component and the analysis of *fluctuating asymmetry* (Palmer & Strobeck, 1986), a constituent of within-individual asymmetric shape component. In organisms with bilateral symmetry, like *P. brassicae*, *fluctuating asymmetry* denotes random deviations from left-right symmetry due to imprecisions in developmental processes (Klingenberg, 2015), and is often studied as a proxy for developmental stability, that is, the ability of an organism to buffer random perturbations of its developmental trajectory (Fusco & Minelli, 2010; Nijhout & Davidowitz, 2003).

## 2 | MATERIALS AND METHODS

This study is based on a longitudinal data set of morphometric and developmental-time measurements on 65 specimens of the lepidopteran *P. brassicae*. The same data set was used in Springolo et al. (in press), to investigate static and ontogenetic variation in size, shape and timing during the larval development of this butterfly. Morphometric data covers the head capsule and includes the first four larval stages (L1–L4). Fifth-stage measurements could have been obtained only by sacrificing the animal at that stage (see Springolo et al. [in press] for details), without means to control for possible extra moults before pupation (and thus for the homology of stages in the sample; Minelli & Fusco, 2013) and successful metamorphosis. Size and shape development were investigated with geometric morphometric methods (Klingenberg, 2015).

### 2.1 | Rearing and collection of exuviae

Larvae were obtained from 19 egg masses deriving from a stock population at the insect farm “Smart Bugs” (Ponzano Veneto, Italy). The larvae were reared individually in petri dishes (Ø 35 mm) and fed ad libitum with a solid-paste mix of vegetables (see David & Gardiner, 1965). The petri dishes were kept in an incubator (Sanyo Versatile Environmental Test Chamber MLR-352H) at constant temperature (25°C), humidity (50% RH) and photoperiod (16L:8D) under the control of an automated system (DAMSystem3 FileScan Software).

Larvae were checked for moult twice a day, approximately 12 h apart, and upon a moult the exuvia of the cephalic capsule was collected and stored in 70% ethanol. Although rearing started from a sample of more than 100 specimens, only data from specimens that completed larval development within five stages, finalized pupal development until adult eclosion and left perfectly preserved exuviae were used.

For details on rearing and exuvia collection, see Springolo et al. (in press).

### 2.2 | Landmark choice and data acquisition

Measurements were taken on the exuviae of the cephalic capsule of larval stages L1–L4. Two parts of the larval head were examined: the plaque formed by the two genae plus the frons (heretofore, *frons*) and the *labrum*. Both parts were analysed through geometric morphometrics (Klingenberg, 2010). Landmarks on the two parts

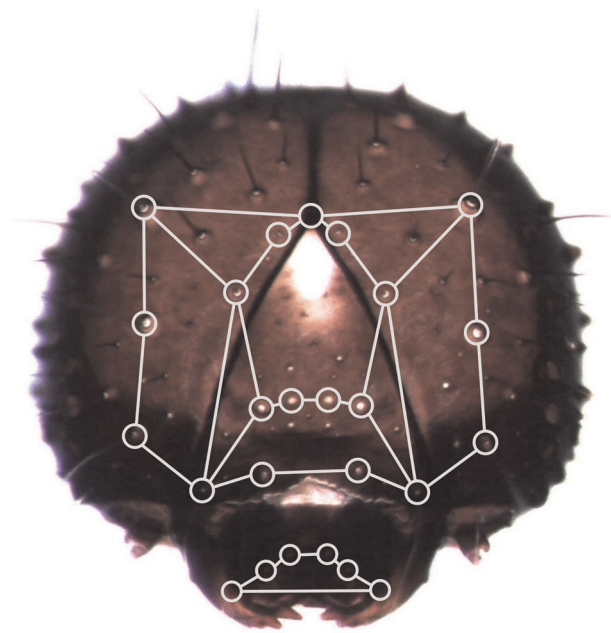


**FIGURE 1** Position of landmarks (circles) on the frons (upper wireframe) and the labrum (lower wireframe) in *Pieris brassicae* larvae

were chosen to be approximately coplanar, to limit error deriving from the projection of a three-dimensional structure onto the plane of the image (Cardini, 2014). One medial landmark was placed at the vertex of the frons, while all the other, two-sided landmarks were positioned in correspondence of the basis of nine pairs of idionymic setae for the frons and three pairs idionymic setae for the labrum (Figure 1). These are setae that are homologous across stages and individuals within a species (Grandjean, 1949). Although the spatial localization of the setae is indicative of size and shape of the sclerites bearing them, their configuration more precisely reflects the topology of the underlying peripheral nervous system (sensory system).

Digital images of the two parts were taken separately for each individual and stage using a digital camera (LEICA DFC 400) mounted on a stereomicroscope (LEICA MZ12.5). Images were acquired through the Leica Application Suite software (V.2.8.1) at the size of  $2048 \times 1536$  pixels. As a standard practice to assess measurement error (Klingenberg, 2015), two images of each part were taken separately for each individual and stage, following a new placement of the specimen under the stereomicroscope. During each placement, the cephalic capsule was temporary glued to the floor of a Petri dish, filled with ethylene glycol to avoid refraction and desiccation, and the latter was aptly oriented to have the part of interest coplanar with focal plane of the microscope. Landmarks were digitized twice on each of the

two images by the same person (AS), in two independent working sessions, using TPSDig 2 (ver. 2.30; Rohlf, 2015). The program tpsUTIL (ver. 1.74; Rohlf, 2015) was used to build the final (.NTS) data files by combining all data into a single data set for each part.

## 2.3 | Morphometric analyses

Both the frons and labrum have *object symmetry*, that is, a form of bilateral symmetry in which a structure is symmetric in itself, and landmark configurations were analysed accordingly (Klingenberg et al., 2002).

Independently for the two parts, configuration of raw coordinates of the landmarks were translated, scaled and rotated through a Generalized Procrustes Superimposition, to obtain a measure of linear size and scale-independent shape coordinates (Rohlf & Slice, 1990). The size of each part was estimated as the centroid size (CS), the square root of the sum of squared distances between each landmark and the centroid of the configuration (Bookstein, 1991). Procrustes methods enable partitioning of shape variation into its symmetric and asymmetric components (Mardia et al., 2000).

Statistical analyses were carried out in MorphoJ (ver. 1.06d; Klingenberg, 2011), Statgraphics Centurion (ver. 18.1.11), R (R Core Team, 2019), and PAST (ver. 3.16; Hammer et al., 2001), as detailed below. Accessory calculations were performed in Microsoft Excel 2010.

### 2.3.1 | Size analyses

Logsize variables in this study are the natural logarithms of the CS of frons and labrum, averaged by individual and stage ( $\ln CS1$ - $\ln CS4$ ). The logarithm of individual per-moult growth rates ( $\ln GR1$ - $\ln GR3$ ) for each of the two parts, corresponding to the postmoult/premoult size ratio at the first, second, and third moult, respectively, were computed as the difference in  $\ln CS$  between successive stages. The logarithm of the individual average per-moult growth rate ( $\ln AGR$ ) was estimated as the arithmetic mean of the three  $\ln GRs$ . This is equal to the logarithm of the geometric mean of the three postmoult/premoult size ratios (Fusco et al., 2012).

Within-individual association between size variables, growth variables and developmental-time variables were investigated by correlation analysis (Pearson's product-moment correlations; implemented in R). Significant results were checked for robustness with the non-parametric Spearman's rank correlation (also implemented in R), which makes no assumption on the linearity of the relationship and the shape of the joint distribution.

We found no inconsistencies between the two analyses. Levene's test for the homogeneity of variances and Fisher's *F* test for the comparison of two variances (implemented in Statgraphics) were used in the analysis of ontogenetic progression of size variance. The latter is more sensitive to nonnormality than the former, however log-transformation of size data made the size distributions of all stages in both parts nonsignificantly deviating from a normal distribution (Shapiro–Wilk's tests, implemented in Statgraphics).

### 2.3.2 | Shape analyses

At the basis of most shape analyses we carried out there is a parametric two-factor general linear model for shape, the Procrustes analysis of variance (Procrustes ANOVA; Klingenberg & McIntyre, 1998; Klingenberg et al., 2002; implemented in MorphoJ), with individuals and sides as the two factors (individuals = random, sides = fixed). This is an extension for shape data of the two-factor ANOVA originally designed for asymmetry analyses of distance measurements (Leamy, 1984; Palmer & Strobeck, 1986). For each part, total shape variation was decomposed into the main effect of “individual” (i.e., variation among individuals—symmetric component), “side” (i.e., directional asymmetry—nonrandom variation between the two sides), the interaction “individual-by-side” (i.e., random variation between the two sides—FA) and measurement error due to digitizing. Procrustes ANOVA assumes that variation is isotropic, that is, equal and independent across all landmarks, which is clearly unrealistic for most biological data (Klingenberg & Monteiro, 2005). However, this analysis is in general more adequate to assess the relative magnitudes of effects in case of object symmetry with respect to the alternative multivariate ANOVA (MANOVA), which does not rest on the isotropic assumption (Klingenberg et al., 2002). We checked for incongruences among the *p* values of MANOVA Pillai's trace statistics (also calculated in MorphoJ) and the *p* values of *F* statistics in Procrustes ANOVA, as a way to detect possible effects deriving from violation of the isotropic assumption (Klingenberg, 2015), and found none (Table S2 in Supporting Information).

The ontogenetic progression of the magnitude of shape variation (both, symmetric and asymmetric components) was tested with the parametric Hartley's test for the equality of variances and Cochran's *C* test, an upper-limit variance outlier test (both implemented in R, package SuppDist). In a multiple sample comparison, Hartley's test computes the ratio of the largest sample variance to the smallest sample

variance, while Cochran's *C* test compares the maximum sample variance to the average sample variance. Both tests are appropriate when sample sizes are all equal (which is the case) and data are nearly normally distributed, a reasonable assumption for intrapopulation shape data, as generally used in studies of asymmetry (Klingenberg, 2015).

Population-level fluctuating asymmetry was estimated through the FA10 index, computed as the square root of the mean squares of the individual-by-side term minus the mean squares of measurement error, adjusted for their appropriate numbers of degrees of freedom (Palmer & Strobeck, 2003). Because FA10 is a variance estimate, FA values were tested with the Hartley's test for the equality of variances.

Individual-level fluctuating asymmetry was estimated as Procrustes FA scores (calculated in MorphoJ). These quantify the amount of fluctuating asymmetry of shape for each individual as the deviations from the mean asymmetry in units of Procrustes distances (Klingenberg & Monteiro, 2005). The progressions of mean and variance of Procrustes FA scores across stages were investigated with a one-way ANOVA with “stage” as single factor followed by a Levene's test for the homogeneity of variances (implemented in Statgraphics). Within-individual association of FA scores in the two head parts and within-individual association between FA scores in each stage were investigated by correlation analysis (Pearson's product-moment correlations; implemented in R).

Between-group Principal Component Analysis (bgPCA) on the asymmetric component of shape (calculated in MorphoJ) was implemented in PAST, using the individual as grouping classification variable. This was followed by a frequency distribution analysis of pairwise Procrustes distances (two-sample Kolmogorov–Smirnov's test), implemented in Statgraphics. Together, the two analyses allowed to visualize and test the ontogenetic variation in the individual pattern of asymmetry in the configuration of landmarks. BgPCA is a multivariate classification technique based on the projection of the data onto the principal components of the group averages. These are orthogonal axes and can be computed even when the data are not of full rank, such as for Procrustes shape coordinates arising in samples of any size, and when covariance matrices are heterogeneous (Mitteroecker & Bookstein, 2011). The two-sample Kolmogorov–Smirnov's test performs a nonparametric test of the null hypothesis that two samples come from the same distribution, by calculating the maximum distance between the two empirical cumulative distributions, with no restrictions about their shape.

### 3 | RESULTS

#### 3.1 | Size regulation

##### 3.1.1 | Compensatory growth: Correlation analysis

Negative correlations between the size at a given stage ( $\ln CS$ ) and the growth rate to the next stage ( $\ln GR$ ) were observed, which provides an indication of compensatory growth. The correlation was negative for all stages in the frons, although significant only at the third stage ( $r = -.47, p = .0001$ ; Figure 2), whereas in the labrum the correlations between  $\ln CS$  and  $\ln GR$  was negative from the second stage on: modest and nonsignificant in L2 ( $r = -.13, p = .31$ ), more consistent and significant in L3 ( $r = -.40, p = .0009$ ; Figure 2).

Size in L4 is positively correlated with both size in L1 ( $\ln CS1$ ) (frons,  $r = .52, p < .0001$ ; labrum,  $r = .58, p < .0001$ ) and the average per-moult growth rate ( $\ln AGR$ ; frons,  $r = .58, p < .0001$ ; labrum,  $r = .79, p < .0001$ ), indicating that both size at hatching and growth rates across ontogeny contributed significantly to individual size variation at the fourth larval stage.

##### 3.1.2 | Compensatory growth: Size variance analysis

Compensatory growth can also be detected as a departure from the expected increase in size variance across ontogeny. For a log-size variable ( $X$ ), the values of within-stage variance in two successive stages ( $i, i + 1$ ) are bound by the following relationship, deriving by the ordinary expression for the variance of the sum of two random variables

$$\text{var}(X_{i+1}) = \text{var}(X_i) + \text{var}(\rho_i) + 2 \cdot \text{cov}(X_i, \rho_i)$$

where  $\rho_i$  is the logarithm of the growth rate of  $X$  between the two stages ( $\rho_i = X_{i+1} - X_i$ ). Assuming non-null  $\text{var}(\rho)$  at each stage, since individuals may have a different genetic makeup and experience different physiological and environmental conditions (see Discussion),  $\text{var}(X)$  tends to increase stage after stage in proportion to  $\text{var}(\rho)$ , unless this is compensated by negative  $\text{cov}(X, \rho)$ .

Centroid size ANOVAs show that measurement error (including both positioning and digitizing) accounts for a minimal fraction of within-stage size variation, 0.1%–0.3% for the frons and 0.3%–1.7% for the labrum

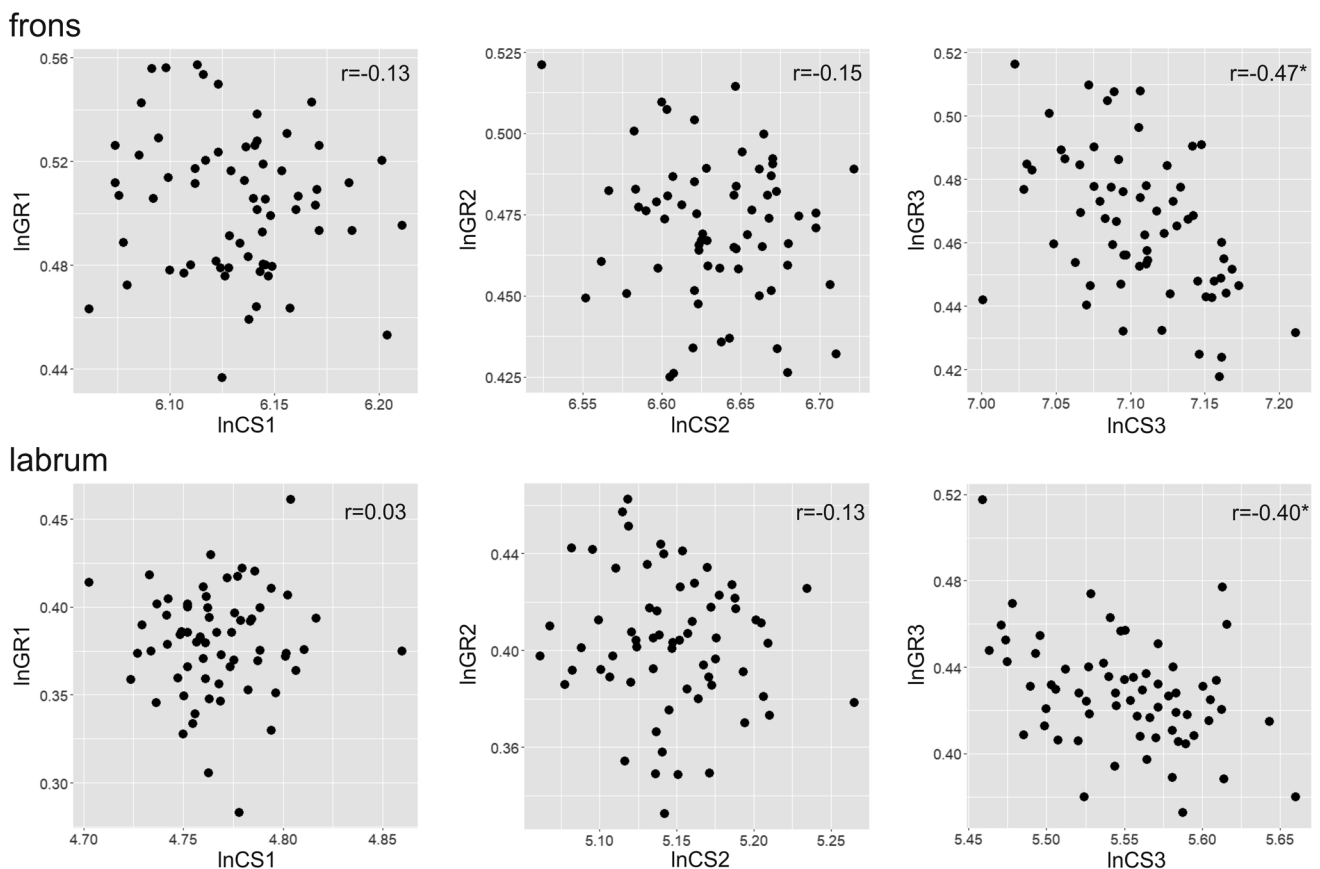
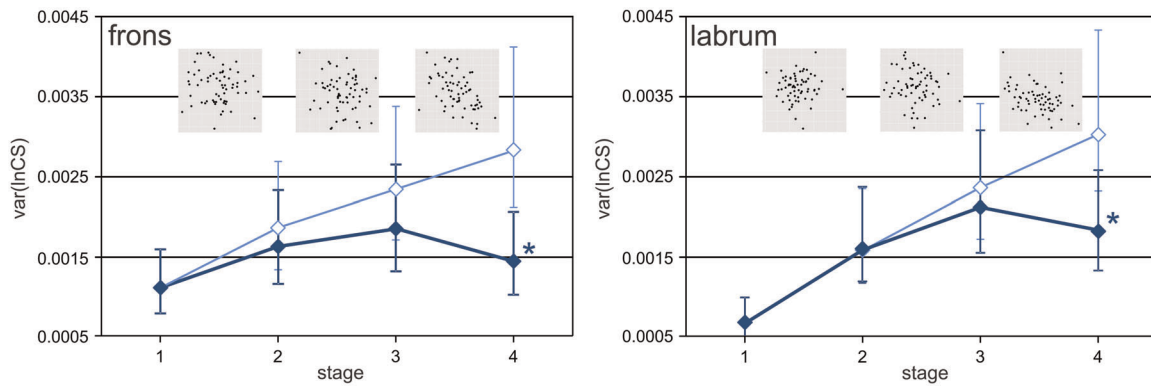


FIGURE 2 Relationship between the size at a given stage ( $\ln CS$ ) and growth rate ( $\ln GR$ ) during the same stage in *Pieris brassicae*, for the frons (upper panels) and the labrum (lower panels). Significantly negative correlations ( $p < .05$ ) are marked with a star



**FIGURE 3** Observed ontogenetic progression of size variance ( $\text{var}(\ln CS)$ , solid diamonds) in *Pieris brassicae*, for the frons (left) and the labrum (right), compared with the expected progression of size variance in the absence of compensatory growth (empty diamonds). Bars are 95% confidence intervals. Significant differences between observed and expected values ( $p < .05$ ) are marked with a star. Inset scatterplots, reproduced from Figure 2, show the effect of the correlation between size ( $\ln CS$ ) and growth rate ( $\ln GR$ ) on compensation at any given stage

(Table S1 in Supporting Information), thus observed variance in each stage is essentially between-individual variance.

In the frons we observed a nonsignificant increase in the size variance across the whole ontogeny (Levene's test,  $W = 1.63$ ,  $p = .1837$ ) and in the labrum the increase in size variance was not significant from the second stage on (Levene's test,  $W = 0.92$ ,  $p = .3992$ ). In the frons only  $\text{var}(\ln CS1)$  and  $\text{var}(\ln CS3)$  are significantly different from each other (Levene's test,  $W = 4.36$ ,  $p = .0387$ ). In the labrum, only  $\text{var}(\ln CS1)$  is significantly different from variance in later stages (Levene's tests,  $p < .0021$ ).

We calculated the expected progression of size variance in the absence of compensation by setting the expected size variance in L1 equal to observed value and adding the observed growth variance at each subsequent stage. This is equivalent to setting  $\text{cov}(\ln CS, \ln GR) = 0$  while maintaining the observed growth parameters. Observed ontogenetic progression of size variance departs markedly from the expected uncompensated progression (Figure 3). There are visible signs of compensation at all stages in the frons and starting from L2 in the labrum, and in both parts the containment of size variance become significant at L4 (one-tailed Fisher's  $F$  test,  $F = 1.99$ ,  $p = .0033$  and  $F = 1.65$ ,  $p = .0240$ , respectively).

### 3.1.3 | Relationship between stage durations and growth rates

There is no evidence of a consistent correlation between stage durations and per-moult growth rates

(Figure 4). Most correlation coefficients are non-significant, except for the positive correlation in L3 for the frons ( $r = .25$ ,  $p = .0417$ ) and the negative correlation in L1 for the labrum ( $r = -.30$ ,  $p = .0137$ ). However, even for these two significant relationships, the amount of variation in growth rate explained by stage duration is modest (6% and 9%, respectively). As a result, both the correlation between cumulative developmental time and average (or cumulative) growth rate across stages (frons,  $r = .04$ ,  $p = .75$ ; labrum  $r = .18$ ,  $p = .16$ ) and the correlation between cumulative developmental time and size at the fourth stage (frons,  $r = .21$ ,  $p = .09$ ; labrum,  $r = .10$ ,  $p = .43$ ) are not significant in either parts.

## 3.2 | Shape regulation

### 3.2.1 | Ontogenetic progression of shape variation: Symmetric component

Depending on the stage, the symmetric component of within-stage shape variation accounts for 67%–69% of total variation (total sum of squares) in the frons and 70%–79% in the labrum. The symmetric component of individual shape variation (variance of the factor “individual” in Procrustes ANOVA) shows no increase across stages in either parts (Figure 5). In the frons, shape variance does not differ significantly across stages (Hartley's test,  $F_{\max} = 1.11$ ,  $p = .31$ ), while in the labrum variance in L1 is significantly larger than those in all subsequent stages (Cochran's  $C$  test,  $C = 0.36$ ,  $p < .0001$ ).

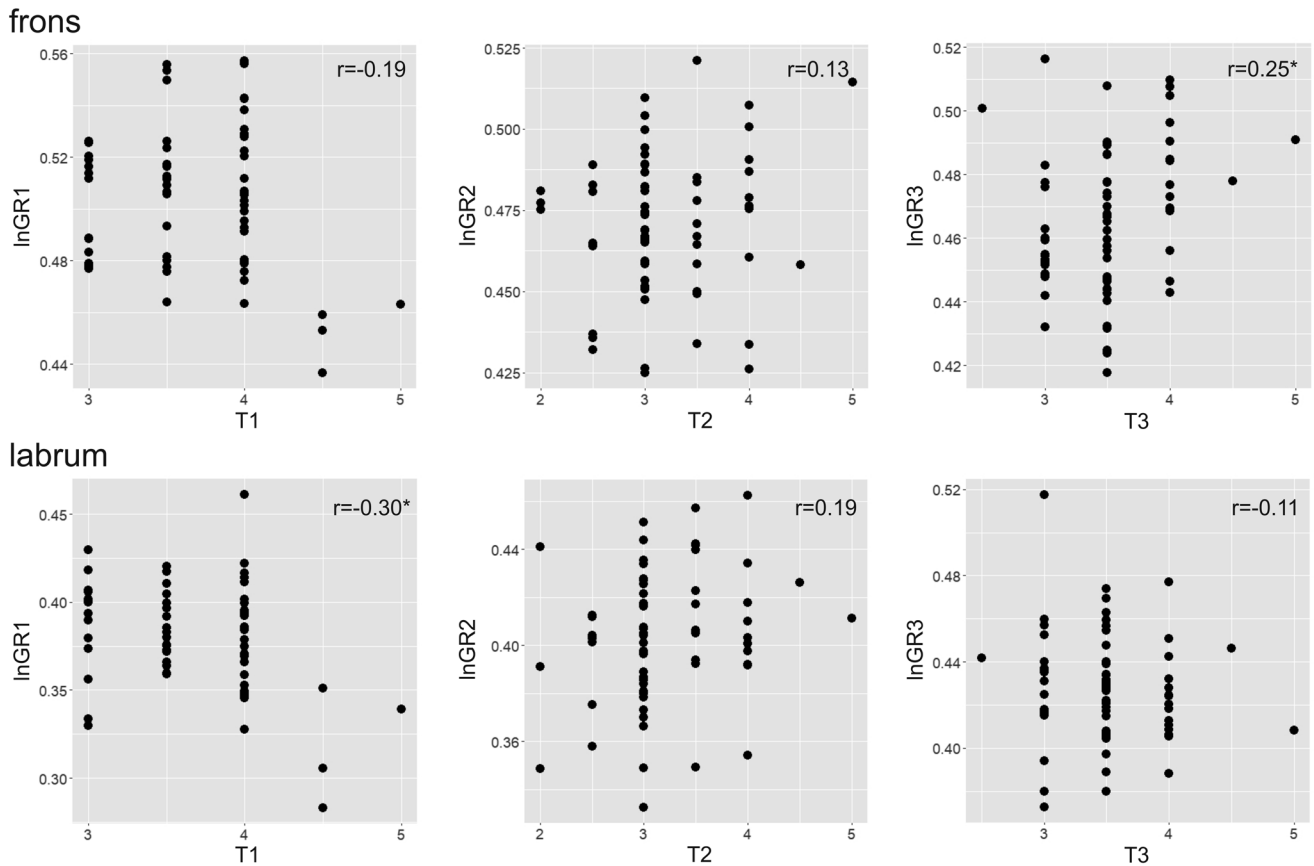


**FIGURE 4** Relationship between the durations of a stage ( $T$ ) in days and the growth rate ( $InGR$ ) during the same stage in *Pieris brassicae*, for the frons (upper panels) and the labrum (lower panels). Significant correlations ( $p < .05$ ) are marked with a star

### 3.2.2 | Ontogenetic progression of fluctuating asymmetry: FA10 index

Procrustes ANOVAs show sizable FA in the larval head shape in all stages and in both parts, as indicated by the significant “individual-by-side” interaction factor ( $p < .0001$ ; Table S2 in Supporting Information). Fluctuating asymmetry in each stage accounts for 89%–94% of total asymmetry variation (sum of squares of factors

“side” + “individual-by-side”) in the frons and for 91%–99% in the labrum, the remaining to be attributed to directional asymmetry (factor “side”).

In both parts, FA10 indexes is fairly constant across stages, in the range 0.0058–0.0062 for the frons and 0.0119–0.0139 for the labrum (Figure 6). In both parts, there are not significant differences in the levels of FA across stages (Hartley’s tests,  $F_{\max} = 1.06$ ,  $p = .78$  and  $F_{\max} = 1.16$ ,  $p = .64$ , respectively).

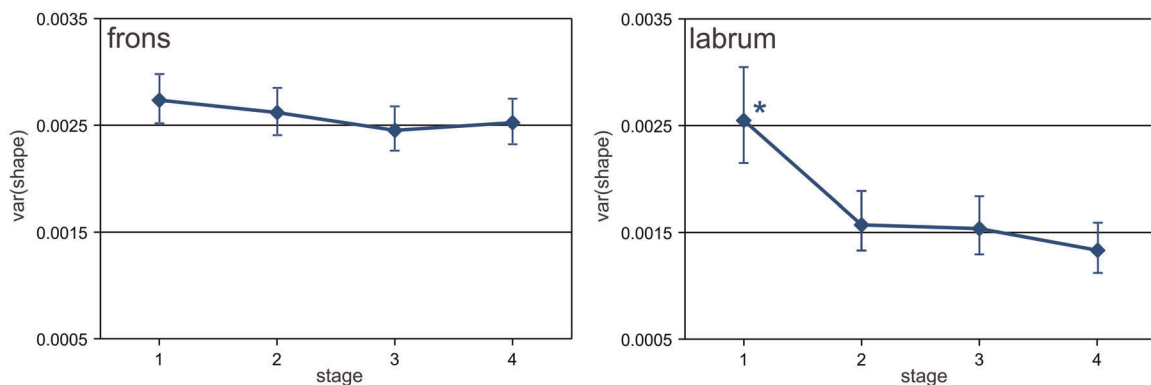


**FIGURE 5** Ontogenetic progression of symmetric shape variance in *Pieris brassicae*, for the frons (left) and the labrum (right). Bars are 95% confidence intervals. Significantly different variances are marked with a star

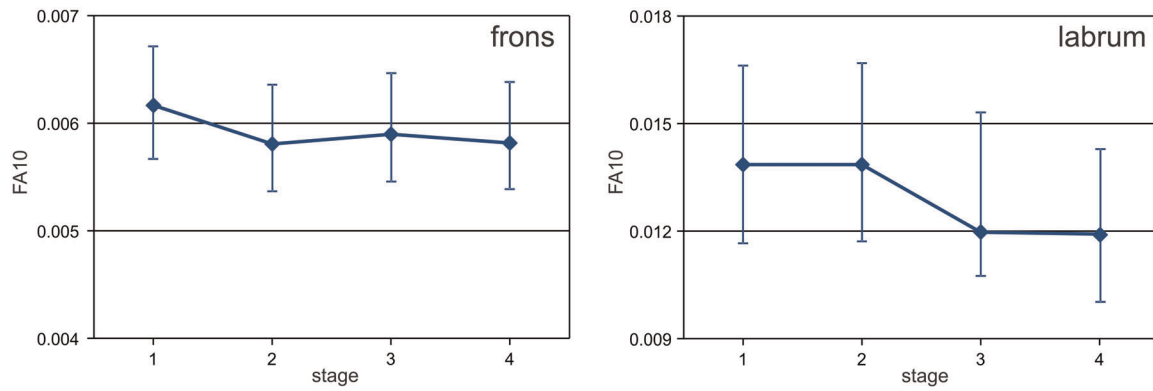


**FIGURE 6** Ontogenetic progression of fluctuating asymmetry (FA10 index) in *Pieris brassicae*, for the frons (left) and the labrum (right). Bars are 95% confidence intervals

### 3.2.3 | Ontogenetic progression of fluctuating asymmetry: Individual Procrustes FA scores

Individual Procrustes FA scores remain fairly constant through ontogeny, both for the frons and the labrum. One-way ANOVAs do not reveal any significant effect of the factor “stage” on the FA scores (frons  $F = 0.77$ ,  $p = .51$ , labrum  $F = 1.92$ ,  $p = .13$ ), and Levene’s tests do not reveal any difference in within-stage variance (frons  $W = 0.05$ ,  $p = .98$ , labrum  $W = 0.89$ ,  $p = .45$ ), confirming FA10 analysis.

Exploiting the longitudinal nature of the data set, it is also evident that individual FA scores in different stages are all positively and significantly correlated (Figure 7), very strongly in the frons ( $r = .73-.94$ ,  $p < .0001$ ), less strongly in the labrum ( $r = .32-.76$ ,  $p < .02$ ), with a tendency for correlation values to become progressively stronger across subsequent stages: L1–L2, L2–L3, L3–L4.

On the contrary, there is no correlation among the individual asymmetry scores in the two parts of the head in any stage ( $r = -.02-.14$ ,  $p = .26-.89$ ). Therefore, although this could result from the simple landmark configuration in the labrum, the value of these scores cannot be interpreted as proxy of the level of developmental buffering at a systemic level, that is, at the level of the whole individual organism.

### 3.2.4 | Ontogenetic progression of fluctuating asymmetry: Landmark configuration

In the frons, bgPCA shows that the asymmetric component of shape during the four larval stages (which is preponderantly fluctuating rather than directional asymmetry, see above) remains confined to relatively small region of the plane of the first two principal

components (accounting for 27.7% and 25.2% of total shape variation, respectively; Figure 8). The difference between the frequency distributions of pairwise Procrustes distances of asymmetric shape component within individuals (i.e., between the four stages of an individual,  $n = 390$ , median = 0.011) and between individuals (i.e., between the individual average shapes across the four stages,  $n = 2080$ , median = 0.026) is highly significant (Kolmogorov–Smirnov’s test,  $D_n = 0.824$ ,  $p < .0001$ ; Figure 9). The labrum has a much simpler landmark configuration than the frons, and group separation in bgPCA (the two first bgPCA components accounting for 48.6% and 23.4% of total shape variation, respectively; Figure 8) is less marked, nonetheless the difference between the frequency distributions of pairwise Procrustes distances within and between individuals is also highly significant ( $D_n = 0.406$ ,  $p < .0001$ ; Figure 9). This means that in both body parts not only the level of asymmetry of an individual remains approximately constant through ontogeny, as seen in the previous section, but also that the specific pattern of asymmetry in the configuration of landmarks does not vary much.

## 4 | DISCUSSION

In Springolo et al. (in press) we analysed several quantitative aspects of growth in *P. brassicae*, in particular with respect to individual variation. In brief, we found that ontogenetic size progression departs modestly, but significantly, from growth at a constant rate (Dyar’s rule), that size at hatching contributes substantially to determine the size of the individual at subsequent stages and that ontogenetic allometry is much more conspicuous than static allometry, the latter in many cases being close to isometry. Here, based on the same longitudinal data set, we found evidence of growth regulatory mechanisms able to restrain size and shape variation,

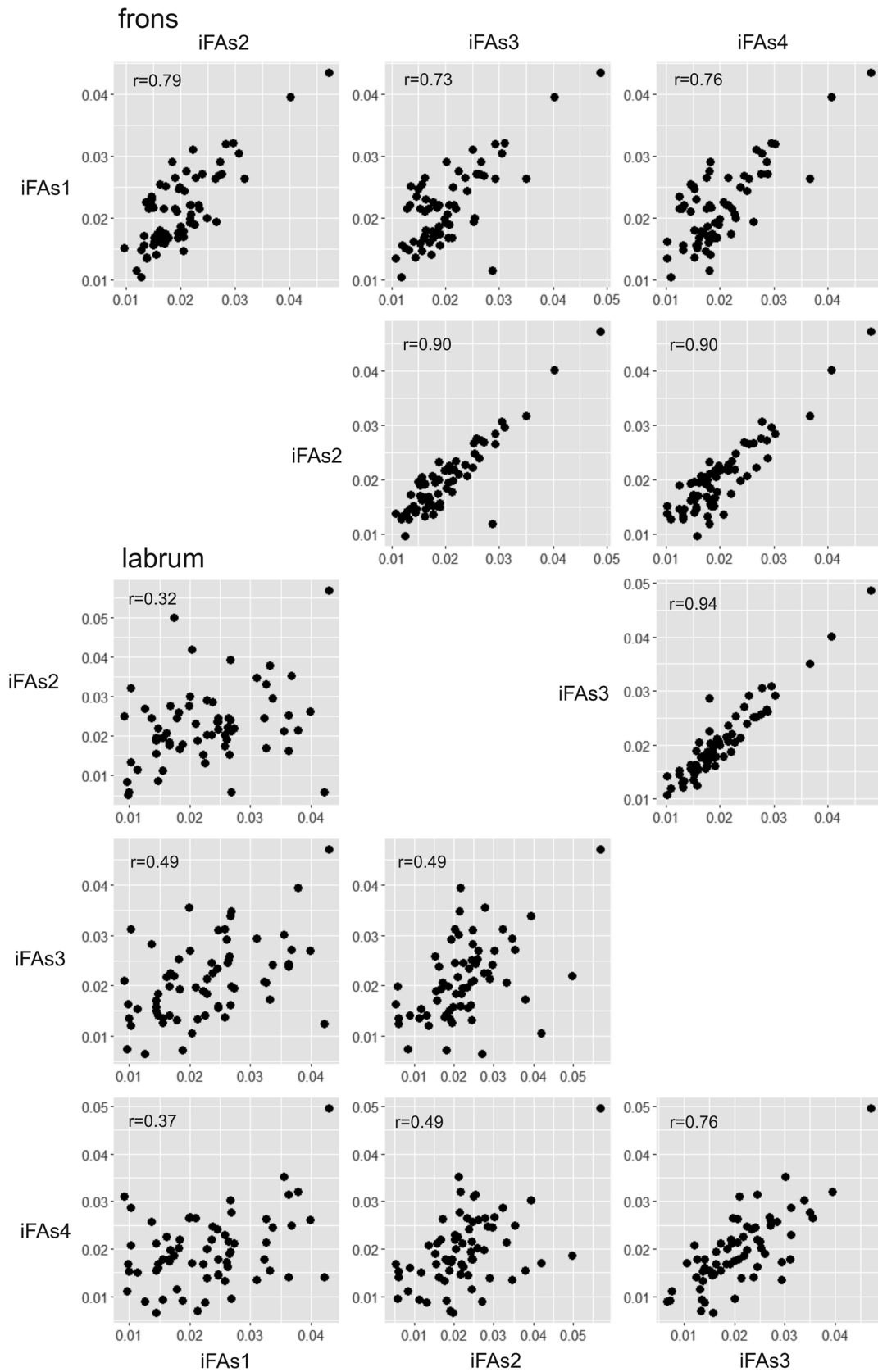


**FIGURE 7** Relationship between individual Procrustes FA scores (iFAs) in different stages (L1–L4) in *Pieris brassicae*, for the frons (upper right panels) and the labrum (lower left panels). Correlations are all statistically significant ( $p < .02$ )

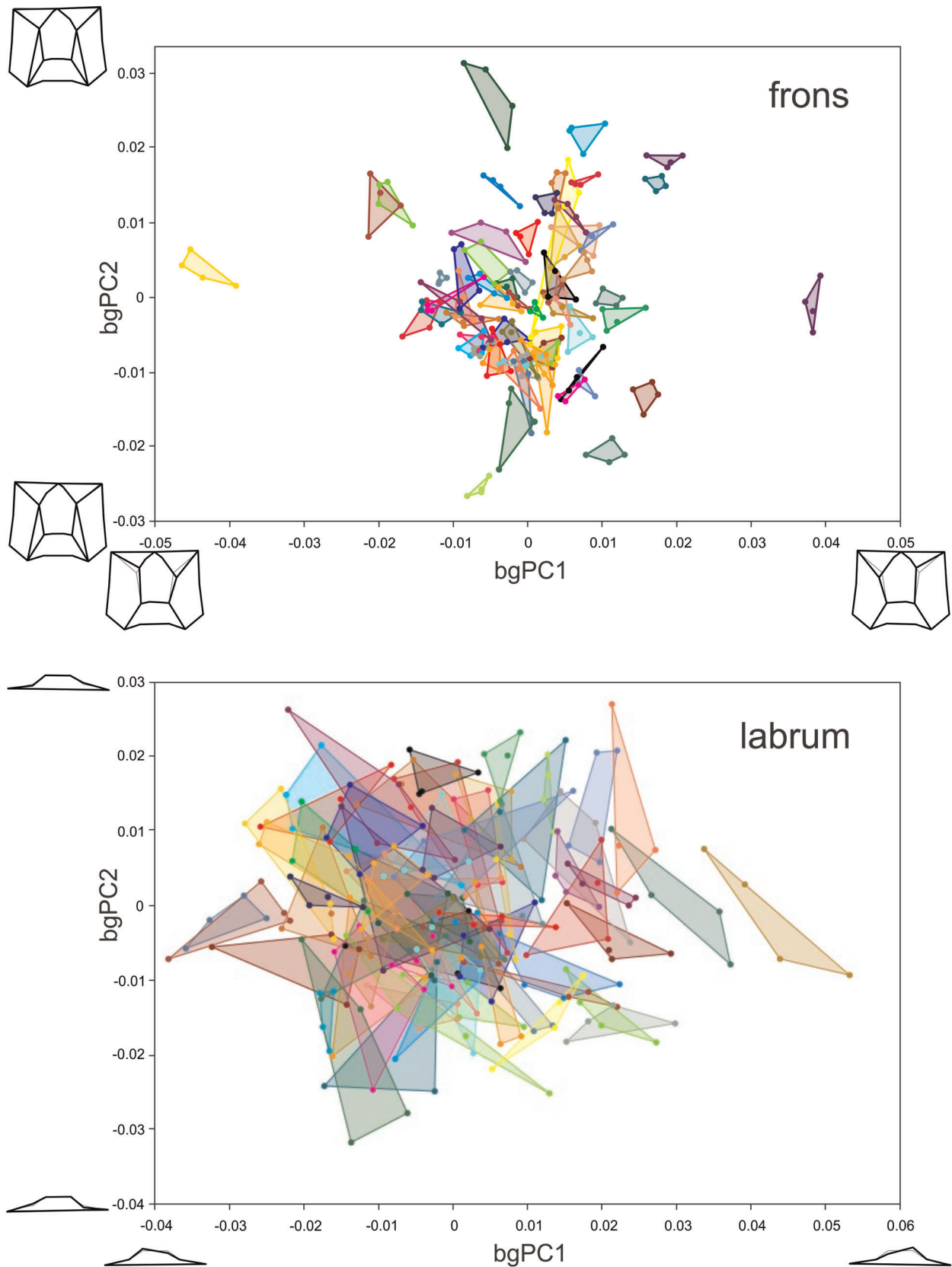
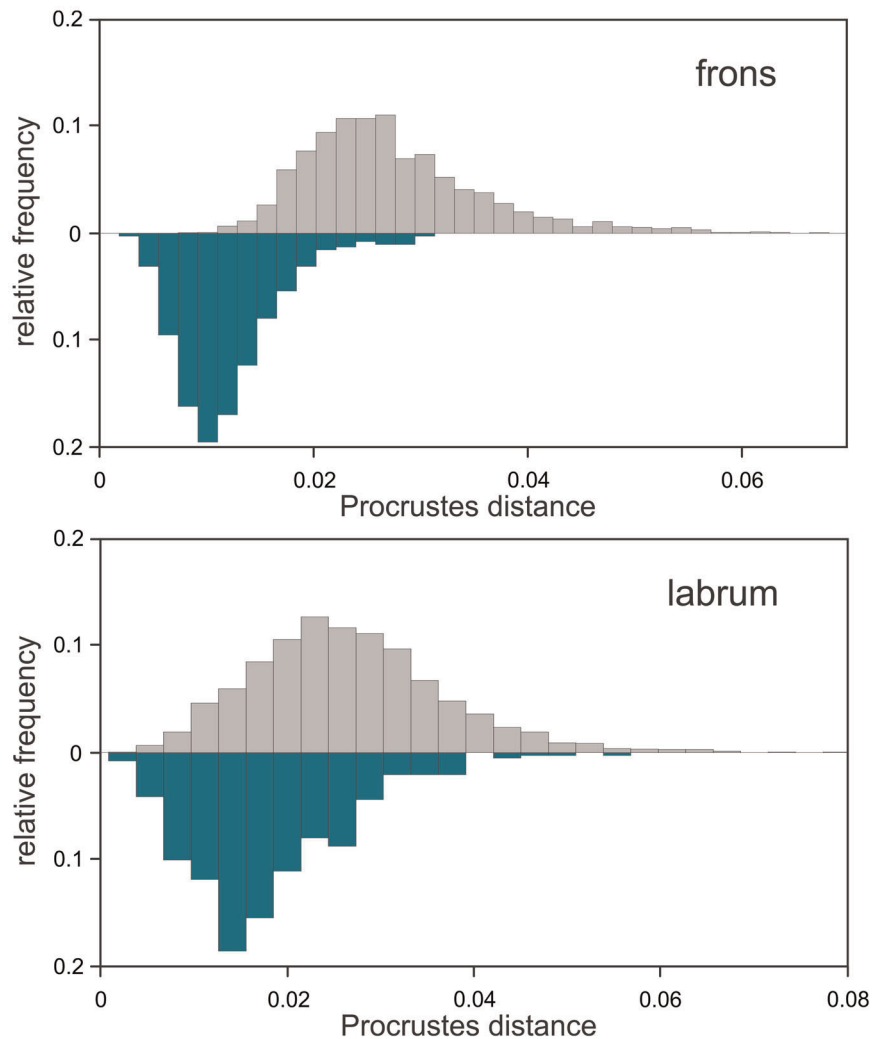


**FIGURE 8** Asymmetric component of the shape in the plane of the first two between-group principal components in *Pieris brassicae*, for the frons (upper panel) and the labrum (lower panel). Minimum convex polygons include the shapes of the four larval stages of each individual. Shape variation along the two axes is shown as thick-line wireframes with respect to the average shape (thin-line wireframes)

**FIGURE 9** Frequency distributions of pairwise Procrustes distances for the asymmetric component of the shape within individuals, that is, between the four stages of an individual, (lower bars,  $n = 390$ ) and between individuals (upper bars,  $n = 2080$ ) in *Pieris brassicae*. For both the frons (upper panel) and the labrum (lower panel) the difference between the two distributions is highly significant ( $p < .0001$ )



including asymmetry, across a growth progression which is four-fold in linear body size and approximately 70-fold in body mass.

#### 4.1 | Compensatory size growth

Both the ontogenetic progression of size variance and the correlation patterns between size at a given stage and growth rate to the next stage show the mark of compensatory growth, although this is not equally effective in all stages and head's parts. Recorded negative correlations are not all statistically significant ( $p < .05$ ), however it should be noted that with a sample size of  $n = 65$ , no correlation smaller than 0.24 can be significant. Nonetheless, compensation even below this magnitude, when protracted for several stages, can result in a significant reduction in size variance in later stages.

Compensation can be partial, when size variance increases by a smaller amount with respect to what would result if growth rates were uncorrelated with size.

However, in *non-longitudinal* datasets (i.e., consisting of data from different individuals at different developmental stages; Cock, 1966) only a complete lack of increase in size variance can be tested and used as an indication of compensatory growth, as any ontogenetic increase in variance could equally result from partial compensation (possibly, associated to high growth rate variances) or from lack of compensation (eventually, associated to low growth rate variances). Here, the longitudinal design of our study allowed to detect and quantify a cumulative level of compensation at the fourth stage in the order of 50% for the frons and 40% for the labrum.

In *P. brassicae*, size compensation is not accomplished through the regulation of developmental timing, but rather through the modulation of per-time growth rate, as there is no consistent pattern of correlation between the duration of a stage and growth rate at the same stage. The non-involvement of timing in size regulation is a bit surprising, since stage durations has a high potential in regulating growth, especially in

holometabolous insects, where the growth of the larva in mass is approximately exponential within a stage (Nijhout et al., 2006) and even relatively small changes in timing can have great impact on body size. However, Klingenberg (1996) found a similar, time-independent size regulation in the waterstrider *Limnoporus canaliculatus* (Heteroptera, Gerridae), although in this bug (but not in *Pieris*; Springolo et al., *in press*) there is also extensive positive correlation among the durations of all larval stages. In insects, the effects of timing on growth are best understood in relation to the size at metamorphosis, which has a direct effect on adult body size (Callier & Nijhout, 2013).

In *P. brassicae*, size compensation is more effective at the third stage, for both investigated parts. This is also the stage at which Springolo et al. (*in press*) recorded a more effective control of cumulative developmental time. Apparently, size and timing go together through a sort of “check point” at this stage, but their compensation is achieved independently. This makes sense from the point of view of developmental regulation as a whole, since there is no positive correlation between size at a given stage and cumulative developmental time until that stage, and an individual can deviate from the target developmental trajectory for the two developmental variables independently. Similar “size check-points” have been described for size regulation of the imago in some insects, as the tobacco hawkmoth *Manduca sexta* (review in Grunert et al., 2015) or the German cockroach *Blattella germanica* (Tanaka, 1981), where however the compensation is attained by altering the number of stages preceding the final moult to adult.

Size regulation by compensatory growth has been documented for several animal taxa, both vertebrate and invertebrates (Riska et al., 1984; Tanner, 1963; Zelditch, 2005). Among arthropods, compensatory growth has been reported in particular among insects and crustaceans (see Minelli & Fusco, 2013 and references therein), and even in a trilobite species (Fusco et al., 2004). In several cases, compensation was observed in some stages but not in others (e.g., Klingenberg, 1996). However, except for a few systems (e.g. *Drosophila*, *Manduca*, among the insects, review in Nijhout, 2008, 2015), the underlying developmental mechanisms are in general poorly understood (Grewal, 2012).

## 4.2 | Regulatory shape change

Neither the variance of the symmetric component of shape, nor the level of fluctuating asymmetry shows any evidence of increase across larval stages, either at the population or individual level. Along with this invariant

magnitude of shape variation across stages, the geometry of individual asymmetry seems to represent a sort of “fingerprint” of the individual. In other words, despite a very large increases in overall body size throughout larval ontogeny, accomplished in discrete steps of growth of about 60% in linear size per stage, and a significant ontogenetic change in the symmetric component of shape (corresponding to ontogenetic allometry; Springolo et al., *in press*), within-stage symmetric shape variance remains constant and the asymmetry present at hatching is basically retained in ontogeny, in terms of both magnitude and geometry.

This stability could partially be explained by the fact that most landmarks correspond to the positions of a set of idionymic setae of the head, that is, the terminals of the peripheral sensory system, which are supposed to be under more strict functional constraints with respect to other cuticular structures. As an alternative, stability could result from pure mechanical constraints during the formation of the new cuticle at each moult cycle, either provided by the connection of the sensilla to the nervous system from inside or by the mould of the old cuticle from outside. Studying the cellular processes involved in the growth of the hypodermis (the epithelium that secretes the cuticle in arthropods) in a centipede, Fusco et al. (2000) found evidence of constraints exerted by the cuticular organules (including sensory setae) on the cuticle shape change across stages.

Whatever the functional explanation, interpreting the observed constancy of symmetric shape variance and shape asymmetry as indicators of compensative development is not as straightforward as in the case of size.

Shape variation, both symmetric and asymmetric, is expected to accumulate across developmental stages, because there are many directions in which variation is possible and deviation in one direction at one stage neither compensates for, nor precludes deviation in other directions at other stages. Thus, unless variation is continually removed, newly arising variation is expected to add to that persisting from earlier stages (Zelditch et al., 2004). However, although there are quantitative models for the expected increase in variance across stages for both size and fluctuating asymmetry of size (in structures with *matching symmetry*, the symmetry of separate left- and right-side paired body structures; Klingenberg et al., 2002), no such models are available for shape. Hence, only a nonsignificant increase in variance can be taken as evidence of shape regulation, with no possibility to detect partial compensation, even in longitudinal data.

Different theoretical models have been proposed to describe and explain ontogenetic variation in FA (Emlen et al., 1993; Kellner & Alford, 2003; Klingenberg, 2003; Swaddle & Witter, 1997), which entail amplification,

constancy or reduction of FA throughout ontogeny (or a section of it). Of particular interest for our case are two models that entail a constancy of FA (Kellner & Alford, 2003). The *persistent asymmetry hypothesis* suggests that departures from symmetry can be determined genetically or through environmental effects early in ontogeny and that these should persist over time, possibly because of the absence of corrective mechanisms (Chippindale & Palmer, 1993). Differently, the *residual asymmetry hypothesis* suggests that there are continuously acting compensatory mechanisms that counter the effects of developmental noise, producing weak or no long-term temporal patterns. Under the latter, the level of asymmetry in each individual would be the residual result of developmental noise minus correction (Van Valen, 1962). It is worth noting, however, that not all the mechanisms conjectured to underlie the two patterns equally apply to structures with object symmetry, like the two structures examined here, as size asymmetry only applies to structures with matching symmetry.

In assessing the case of *P. brassicae* with respect to these two hypotheses, it is worth remarking here the distinction between two different developmental mechanisms through which regulation can be implemented, namely *control* and *compensation*. Control entails absence of deviation, through a mechanism that prevents deviations to appear. Compensation entails that deviations from a target are followed by error correction. In vertebrates, growth is continuous, and compensation could be detected, for instance, in the oscillation of asymmetry at different developmental times (Kellner & Alford, 2003). In arthropods, which have stepwise growth, this is observable in the exoskeleton only if compensation operates from one stage to another, but within-stage compensation is not distinguishable from control. In *P. brassicae*, correlation analysis of individual FA scores provides no evidence for between-stage compensation. However, if the expectation in the absence of regulation is an increase of symmetric shape variance and FA along ontogeny, observed ontogenetic patterns show the signature of within-stage regulation, either in the form of compensation or control (or both). Note that symmetric shape variance and FA are not only geometrically independent, they can also be independently regulated, as shown by the ontogenetic decrease in shape variance associated to an increase of FA recorded in primate skeletal traits (Hallgrímsson, 1999).

Previous studies on the ontogeny of FA, reporting on different species and characters, gave contradictory results. Some studies documented an increase in the amount of FA during growth (e.g., Hallgrímsson, 1993; Servia et al., 2002), other studies reported constant levels of FA during growth, in agreement with what has been

found in this study (e.g., Chippindale & Palmer, 1993; Stige et al., 2006; Willmore et al., 2006), and still others recorded an ontogenetic decrease of FA (Tomkins, 1999). Lazić et al. (2017) found constant asymmetry across the age range in two lizard species, but an increase with age in a third. Further comparative data needs to be collected before venturing in any attempt of generalization.

### 4.3 | Concluding remarks

Although longitudinal studies can dissect growth patterns very accurately to access detailed quantitative aspects of growth regulation, size and shape control and compensation in laboratory animals is likely to differ from those in natural populations, due to the greater heterogeneity of environmental conditions in the wild (Willmore et al., 2006). Two opposite deviations from what is observed under laboratory condition could occur. The mechanism of compensation might prove insufficient to effectively limit environmental variation effects, with the result of an increase of size and/or shape variance across ontogeny. On the contrary, certain regulatory mechanisms, undetected in laboratory conditions because they need stronger environmental stimuli to operate, might be activated as a response of the more effective stimuli in the wild.

Another important difference between laboratory and field studies, is that under controlled laboratory condition, to a large extent, only *developmental stability* mechanisms buffering against developmental noise (*around* the target phenotype) are expected to operate, while under natural conditions these are expected to operate in concert with *canalization* mechanisms, to reduce environmental effects on the reaction norm (Fusco & Minelli, 2010). There has been a debate on whether the buffering processes involved in canalization and developmental stability are the same or they are distinct (Debat et al., 2000; Hallgrímsson et al., 2002; Klingenberg, 2019), but the design of our experiment does not allow to investigate this relationship, and our results are clearly concerned mainly with the latter.

In conclusion, the larval development of *P. brassicae* shows the mark of several forms of developmental regulation, which, judging by the differences in the ontogenetic progressions of size and shape variation and the patterns of developmental character correlations, exhibit a certain degree of independence from each other. However, further studies, broadening the taxonomic coverage, taking into consideration a variety of morphological features and possibly combining laboratory and field observations, will be necessary for a better understanding of the

regulatory phenomena during growth and their influence on phenotypic evolution.

## ACKNOWLEDGMENTS

This study has been supported by a grant from the Italian Ministry of Education, University and Research (MIUR) to GF. We thank Emiliano Peretti for assistance with bgPCA and Alessandro Minelli and three anonymous referees for insightful comments on a previous version of the article.

## CONFLICT OF INTERESTS

The authors declare that there are no conflict of interests.

## DATA AVAILABILITY STATEMENT

The datasets supporting this article have been uploaded to Dryad (<https://doi.org/10.5061/dryad.s4mw6m95h>).

## ORCID

Giuseppe Fusco  <http://orcid.org/0000-0002-4690-6049>

## REFERENCES

- Bookstein, F. L. (1991). *Morphometric tools for landmark data. Geometry and biology*. Cambridge University Press.
- Bruijning, M., Metcalf, C. J. E., Jongejans, E., & Ayroles, J. F. (2020). The evolution of variance control. *Trends in Ecology & Evolution*, *35*, 22–33.
- Callier, V., & Nijhout, H. F. (2013). Body size determination in insects: A review and synthesis of size- and brain-dependent and independent mechanisms. *Biological Reviews*, *88*, 944–954.
- Cardini, A. (2014). Missing the third dimension in geometric morphometrics: How to assess if 2D images really are a good proxy for 3D structures? *Hystrix*, *25*, 63–72.
- Chippindale, A. K., & Palmer, A. R. (1993). Persistence of subtle departures from symmetry over multiple molts in individual Brachyuran crabs: Relevance to developmental stability. *Genetica*, *89*, 185–199.
- Cock, A. G. (1966). Genetical aspects of metrical growth and form in animals. *The Quarterly Review of Biology*, *41*, 131–190.
- David, W. A. L., & Gardiner, B. O. C. (1965). Rearing *Pieris brassicae* L. larvae on semi-synthetic diets. *Nature*, *207*, 882–883.
- Debat, V., Alibert, P., David, P., Paradis, E., & Auffray, J.-C. (2000). Independence between developmental stability and canalization in the skull of the house mouse. *Proceedings of the Royal Society B*, *267*, 423–430.
- Emlen, J. M., Freeman, D. C., & Graham, J. H. (1993). Nonlinear growth dynamics and the origin of fluctuating asymmetry. *Genetica*, *89*, 77–96.
- Fusco, G. (2001). How many processes are responsible for phenotypic evolution? *Evolution & Development*, *3*, 279–286.
- Fusco, G., Brena, C., & Minelli, A. (2000). Cellular processes in the growth of lithobiomorph centipedes (Chilopoda: Lithobiomorpha). A cuticular view. *Zoologischer Anzeiger*, *239*, 91–102.
- Fusco, G., Garland, T., Jr., Hunt, G., & Hughes, N. C. (2012). Exploring developmental trait evolution in trilobites. *Evolution*, *66*, 314–329.
- Fusco, G., Hughes, N. C., Webster, M., & Minelli, A. (2004). Exploring developmental modes in a fossil arthropod: Growth and trunk segmentation of the trilobite *Aulacopleura konincki*. *The American Naturalist*, *163*, 167–183.
- Fusco, G., & Minelli, A. (2010). Phenotypic plasticity in development and evolution: Facts and concepts. *Philosophical Transactions of the Royal Society B*, *365*, 547–556.
- Grandjean, F. (1949). Au sujet des variations individuelles et des polygones de fréquence. *Comptes rendus hebdomadaires des séances de l'Académie des sciences*, *229*, 801–804.
- Grewal, S. S. (2012). Controlling animal growth and body size: Does fruit fly physiology point the way? *F1000 Biology Reports*, *4*, 12.
- Grunert, L. W., Clarke, J. W., Ahuja, C., Eswaran, H., & Nijhout, H. F. (2015). A quantitative analysis of growth and size regulation in *Manduca sexta*: The physiological basis of variation in size and age at metamorphosis. *PLOS One*, *10*, e0127988.
- Hallgrímsson, B. (1993). Fluctuating asymmetry in *Macaca fascicularis*: A study of the etiology of developmental noise. *International Journal of Primatology*, *14*, 421–443.
- Hallgrímsson, B. (1999). Ontogenetic patterning of skeletal fluctuating asymmetry in rhesus macaques and humans: Evolutionary and developmental implications. *International Journal of Primatology*, *20*, 121–151.
- Hallgrímsson, B., Willmore, K., & Hall, B. K. (2002). Canalization, developmental stability, and morphological integration in primate limbs. *The American Journal of Physical Anthropology*, *119*, 131–158.
- Hammer, Ø., Harper, D. A. T., & Ryan, P. D. (2001). PAST: Paleontological statistics software package for education and data analysis. *Palaeontologia Electronica*, *4*, 4.
- Hartnoll, R. G. (1982). Growth. In D. E. Bliss (Ed.), *The Biology of Crustacea* (Vol. 2, pp. 111–196). Academic Press.
- Kellner, J. R., & Alford, R. A. (2003). The ontogeny of fluctuating asymmetry. *The American Naturalist*, *161*, 931–947.
- Klingenberg, C. P. (1996). Individual variation of ontogenies: A longitudinal study of growth and timing. *Evolution*, *50*, 2412–2428.
- Klingenberg, C. P. (2003). A developmental perspective on developmental instability: Theory, models, and mechanisms. In M. Polak (Ed.), *Developmental instability: Causes and consequences* (pp. 14–34). Oxford University Press.
- Klingenberg, C. P. (2010). Evolution and development of shape: Integrating quantitative approaches. *Nature Reviews Genetics*, *11*, 623–635.
- Klingenberg, C. P. (2011). MorphoJ: An integrated software package for geometric morphometrics. *Molecular Ecology Resources*, *11*, 353–357.
- Klingenberg, C. P. (2015). Analyzing fluctuating asymmetry with geometric morphometrics: Concepts, methods, and applications. *Symmetry*, *7*, 843–934.
- Klingenberg, C. P. (2019). Phenotypic plasticity, developmental instability, and robustness: The concepts and how they are connected. *Frontiers in Ecology & Evolution*, *7*, 56.
- Klingenberg, C. P., Barluenga, M., & Meyer, A. (2002). Shape analysis of symmetric structures: Quantifying variation among individuals and asymmetry. *Evolution*, *56*, 1909–1920.
- Klingenberg, C. P., & McIntyre, G. S. (1998). Geometric morphometrics of developmental instability: Analyzing patterns of fluctuating asymmetry with Procrustes methods. *Evolution*, *52*, 1363–1375.

- Klingenberg, C. P., & Monteiro, L. R. (2005). Distances and directions in multidimensional shape spaces: Implications for morphometric applications. *Systematic Biology*, *54*, 678–88.
- Lazić, M. M., Rödder, D., & Kaliontzopoulou, A. (2017). The ontogeny of developmental buffering in lizard head shape. *Evolution & Development*, *19*, 244–252.
- Leamy, L. (1984). Morphometric studies in inbred and hybrid house mice. V. Directional and fluctuating asymmetry. *The American Naturalist*, *123*, 579–593.
- Mardia, K. V., Bookstein, F. L., & Moreton, I. J. (2000). Statistical assessment of bilateral symmetry of shapes. *Biometrika*, *87*, 285–300.
- Minelli, A., & Fusco, G. (2013). Arthropod post-embryonic development. In A. Minelli, G. Boxshall, & G. Fusco (Eds.), *Arthropod biology and evolution. Molecules, development, morphology* (pp. 91–122). Springer Verlag.
- Mitteroecker, P., & Bookstein, F. (2011). Linear discrimination, ordination, and the visualization of selection gradients in modern morphometrics. *Evolutionary Biology*, *38*, 100–114.
- Nijhout, H. F. (2008). Size matters (but so does time), and it's OK to be different. *Developmental Cell*, *15*, 491–492.
- Nijhout, H. F. (2015). Big or fast: Two strategies in the developmental control of body size. *BMC Biology*, *13*, 57.
- Nijhout, H. F., & Callier, V. (2015). Developmental mechanisms of body size and wing-body scaling in insects. *Annual Review of Entomology*, *60*, 141–56.
- Nijhout, H. F., & Davidowitz, G. (2003). Developmental perspectives on phenotypic variation, canalization, and fluctuating asymmetry. In M. Polak (Ed.), *Developmental instability: Causes and consequences* (pp. 3–13). Oxford University Press.
- Nijhout, H. F., Davidowitz, G., & Roff, D. A. (2006). A quantitative analysis of the mechanism that controls body size in *Manduca sexta*. *Journal of Biology*, *5*, 16.
- Palmer, A. R., & Strobeck, C. (1986). Fluctuating asymmetry: Measurement, analysis, patterns. *The Annual Review of Ecology, Evolution, & Systematics*, *17*, 391–421.
- Palmer, A. R., & Strobeck, C. (2003). Fluctuating asymmetry analysis revisited. In M. Polak (Ed.), *Developmental instability: Causes and consequences* (pp. 279–319). Oxford University Press.
- R Core Team. (2019). *R: A language and environment for statistical computing*. R Foundation for Statistical Computing. <http://www.R-project.org/>
- Riska, B., Atchley, W. R., & Rutledge, J. J. (1984). A genetic analysis of targeted growth in mice. *Genetics*, *107*, 79–101.
- Roff, D. A. (1992). *The evolution of life histories*. Chapman & Hall.
- Rohlf, F. J. (2015). The tps series of software. *Hystrix*, *26*, 9–12.
- Rohlf, F. J., & Slice, D. (1990). Extensions of the Procrustes method for the optimal superimposition of landmarks. *Systematic Biology*, *39*, 40–59.
- Servia, M. J., Cobo, F., & Gonzalez, M. A. (2002). Ontogeny of individual asymmetries in several traits of larval *Chironomus riparius* Meigen, 1804 (Diptera, Chironomidae). *Canadian Journal of Zoology*, *80*, 1470–1479.
- Shingleton, A. W. (2010). The regulation of organ size in *Drosophila*. Physiology, plasticity, patterning and physical force. *Organogenesis*, *6*, 76–87.
- Springolo, A., Rigato, E., & Fusco, G. (in press). Larval growth and allometry in the cabbage butterfly *Pieris brassicae* (Lepidoptera: Pieridae). *Acta Zoologica*. <https://doi.org/10.1111/azo.12317>
- Stige, L. C., Hessen, D. O., & Vøllestad, L. A. (2006). Fitness, developmental instability, and the ontogeny of fluctuating asymmetry in *Daphnia magna*. *Biological Journal of the Linnean Society*, *88*, 179–192.
- Swaddle, J. P., & Witter, M. S. (1997). On the ontogeny of developmental stability in a stabilized trait. *Proceedings of the Royal Society B*, *264*, 329–334.
- Tanaka, A. (1981). Regulation of body size during larval development in the German cockroach, *Blattella germanica*. *Journal of Insect Physiology*, *27*, 587–592.
- Tanner, J. M. (1963). Regulation of growth in size in mammals. *Nature*, *199*, 845–850.
- Tomkins, J. L. (1999). The ontogeny of asymmetry in earwig forceps. *Evolution*, *53*, 157–163.
- Van Dongen, S. (2006). Fluctuating asymmetry and developmental instability in evolutionary biology: Past, present and future. *Journal of Evolutionary Biology*, *19*, 1727–1743.
- Van Valen, L. (1962). A study of fluctuating asymmetry. *Evolution*, *16*, 125–142.
- Willmore, K. E., Leamy, L., & Hallgrímsson, B. (2006). Effects of developmental and functional interactions on mouse cranial variability through late ontogeny. *Evolution & Development*, *8*, 550–567.
- Zelditch, M. L. (2005). Developmental regulation of variability. In B. Hallgrímsson, & B. K. Hal (Eds.), *Variation: A central concept in biology* (pp. 249–273). Elsevier.
- Zelditch, M. L., Lundrigan, B. L., & Garland, T., Jr. (2004). Developmental regulation of skull morphology. I. Ontogenetic dynamics of variance. *Evolution & Development*, *6*, 194–206.

## SUPPORTING INFORMATION

Additional Supporting Information may be found online in the supporting information tab for this article.

**How to cite this article:** Fusco G, Rigato E, Springolo A. Size and shape regulation during larval growth in the lepidopteran *Pieris brassicae*. *Evolution & Development*. 2021;23:46–60. <https://doi.org/10.1111/ede.12362>

# Size and shape regulation during larval growth in the lepidopteran *Pieris brassicae*

Giuseppe Fusco, Emanuele Rigato, Arianna Springolo

## Supporting information

**Table S1.** Centroid size ANOVAs of frons and labrum in the first four larval stages of *P. brassicae*. SS, sum of squares; MS mean squares; df, degrees of freedom; F, Fisher's F statistic; p, parametric p-value. Significant p-values ( $p < 0.05$ ) are in bold.

FRONS size					
Stage 1	SS	MS	df	F	p
Individual	60541.25	945.96	64	1000.90	<b>&lt;0.0001</b>
Residual	184.30	0.95	195		
Stage 2	SS	MS	df	F	p
Individual	239423.06	3740.99	64	1292.71	<b>&lt;0.0001</b>
Residual	564.31	2.89	195		
Stage 3	SS	MS	df	F	p
Individual	699503.52	10929.74	64	2054.29	<b>&lt;0.0001</b>
Residual	1037.49	5.32	195		
Stage 4	SS	MS	df	F	p
Individual	1359899.14	21248.42	64	1453.47	<b>&lt;0.0001</b>
Residual	2850.72	14.62	195		
LABRUM size					
Stage 1	SS	MS	df	F	p
Individual	2434.00	38.03	64	180.53	<b>&lt;0.0001</b>
Residual	41.08	0.21	195		
Stage 2	SS	MS	df	F	p
Individual	12524.00	195.69	64	530.77	<b>&lt;0.0001</b>
Residual	71.89	0.37	195		
Stage 3	SS	MS	df	F	p
Individual	35966.06	561.97	64	726.07	<b>&lt;0.0001</b>
Residual	150.93	0.77	195		
Stage 4	SS	MS	df	F	p
Individual	73542.09	1149.10	64	954.94	<b>&lt;0.0001</b>
Residual	234.65	1.20	195		

**Table S2.** Procrustes ANOVAs of frons and labrum shape in the first four larval stages of *P. brassicae*. SS, sum of squares; MS mean squares; df, degrees of freedom; F, Fisher's F statistic; p, parametric p-value. MANOVA Pillai's trace statistic (PT) and the associated parametric p-value (PTp) are shown for comparison. Significant p-values ( $p < 0.05$ ) are in bold. For details on the calculation of the degrees of freedom, deriving from the corresponding shape dimensions, see Table 1 in Klingenberg, Barluenga & Meyer (2002).

FRONS shape							
Stage 1	SS	MS	df	F	p	PT	PTp
Individual	0.2980	0.0003	1088	2.27	<b>&lt;0.0001</b>	16.54	<b>&lt;0.0001</b>
Side	0.0085	0.0005	17	4.13	<b>&lt;0.0001</b>	0.60	<b>&lt;0.0001</b>
Individual x Side	0.1314	0.0001	1088	138.42	<b>&lt;0.0001</b>	16.17	<b>&lt;0.0001</b>
Residual	0.0058	8.72E-07	6630				
Stage 2	SS	MS	df	F	p	PT	PTp
Individual	0.2852	2.62E-04	1088	2.45	<b>&lt;0.0001</b>	16.67	<b>&lt;0.0001</b>
Side	0.0077	4.53E-04	17	4.24	<b>&lt;0.0001</b>	0.67	<b>&lt;0.0001</b>
Individual x Side	0.1163	1.07E-04	1088	216.54	<b>&lt;0.0001</b>	16.61	<b>&lt;0.0001</b>
Residual	0.0033	4.49E-07	6630				
Stage 3	SS	MS	df	F	p	PT	PTp
Individual	0.2679	2.46E-04	1088	2.24	<b>&lt;0.0001</b>	16.78	<b>&lt;0.0001</b>
Side	0.0108	6.35E-04	17	5.77	<b>&lt;0.0001</b>	0.64	<b>&lt;0.0001</b>
Individual x Side	0.1198	1.10E-04	1088	254.05	<b>&lt;0.0001</b>	16.72	<b>&lt;0.0001</b>
Residual	0.0029	4.33E-07	6630				
Stage 4	SS	MS	df	F	p	PT	PTp
Individual	0.2750	2.53E-04	1088	2.36	<b>&lt;0.0001</b>	16.80	<b>&lt;0.0001</b>
Side	0.0144	8.46E-04	17	7.90	<b>&lt;0.0001</b>	0.82	<b>&lt;0.0001</b>
Individual x Side	0.1165	1.07E-04	1088	280.51	<b>&lt;0.0001</b>	16.64	<b>&lt;0.0001</b>
Residual	0.0025	3.82E-07	6630				
LABRUM shape							
Stage 1	SS	MS	df	F	p	PT	PTp
Individual	0.6511	0.0025	256	4.16	<b>&lt;0.0001</b>	3.93	<b>&lt;0.0001</b>
Side	0.0028	0.0007	4	1.15	0.335	0.05	0.529
Individual x Side	0.1565	0.0006	256	78.62	<b>&lt;0.0001</b>	3.92	<b>&lt;0.0001</b>
Residual	0.0121	7.77E-06	1560				
Stage 2	SS	MS	df	F	p	PT	PTp
Individual	0.4028	0.0016	256	2.57	<b>&lt;0.0001</b>	3.94	<b>&lt;0.0001</b>
Side	0.0017	0.0004	4	0.71	0.585	0.07	0.328
Individual x Side	0.1564	0.0006	256	89.65	<b>&lt;0.0001</b>	3.88	<b>&lt;0.0001</b>
Residual	0.0106	6.82E-06	1560				
Stage 3	SS	MS	df	F	p	PT	PTp
Individual	0.3930	0.0015	256	2.97	<b>&lt;0.0001</b>	3.94	<b>&lt;0.0001</b>
Side	0.0040	0.0010	4	1.93	0.106	0.15	0.059
Individual x Side	0.1325	0.0005	256	80.03	<b>&lt;0.0001</b>	3.86	<b>&lt;0.0001</b>
Residual	0.0101	6.47E-06	1560				
Stage 4	SS	MS	df	F	p	PT	PTp
Individual	0.3419	0.0013	256	2.95	<b>&lt;0.0001</b>	3.94	<b>&lt;0.0001</b>
Side	0.0113	0.0028	4	6.26	<b>&lt;0.0001</b>	0.40	<b>&lt;0.0001</b>
Individual x Side	0.1159	0.0005	256	78.26	<b>&lt;0.0001</b>	3.82	<b>&lt;0.0001</b>
Residual	0.0090	5.78E-06	1560				